

Spangler, E.¹, Hubbard, T.D.¹, Daanen, R.P.¹, Darrow, M.M.², Simpson, J.M.², and Southerland, L.²

¹ Alaska Division of Geological & Geophysical Surveys, 3354 College Rd., Fairbanks, AK 99709
² Mining and Geological Engineering Department, University of Alaska Fairbanks, Box 755800, Fairbanks, AK 99775

1. ABSTRACT

Frozen debris lobes (debris mass-movement features on permafrost slopes) are present along the Dalton Highway corridor in the southern Brooks Range, Alaska. Active downslope movement of these features presents potential hazards and geologic-engineering challenges to the highway as well as the adjacent Trans Alaska Pipeline System. To better characterize frozen debris lobes and assess their associated geologic hazards, we initiated a focused study along a 20-mile stretch of the Dalton Highway between Wiseman and Chandalar Shelf. Here we present observations of the bedrock geology and geomorphology of eight frozen debris lobe catchments, based on ArcGIS analysis of multi-date remotely sensed imagery and 2013 summer field work.

Preliminary results indicate that frozen debris lobes form in gullies, cored by less-competent material such as phyllite, slate, and chloritic schist and flanked by ridges of competent bedrock such as limestone, marble, metasediment, and gneiss. Catchment areas are characterized by solifluction lobes, fractures, slumps, channels, standing water, permafrost, and minimal vegetative cover. Debris is contributed to the frozen debris lobes by a variety of slope processes, including solifluction, rockfall, slope failure, and runoff. Characterizing the geologic attributes of the catchment area is an important component to understanding the hazard potential of the frozen debris lobes. Our observations and results will provide new information useful for maintenance of current infrastructure and planning for future development in the corridor.

2. INTRODUCTION

In the south-trending Dietrich River Valley of the south-central Brooks Range of Alaska, USA, are a series of frozen debris lobes that pose potential geologic hazards and maintenance issues for transportation and resource infrastructure connecting Interior Alaska with the North Slope (Figure 1A). These frozen debris lobes are located along the Dalton Highway transportation corridor, the adjacent Trans Alaska Pipeline System, and a proposed natural gas pipeline about 40 km north of Wiseman (Figure 1B). The frozen debris lobes are actively sliding features and impacting infrastructure (Daanen et al., 2012; Darrow et al., 2012) (Figure 1C).

The Alaska Division of Geological & Geophysical Surveys (DGGS) and the University of Alaska Fairbanks, are conducting an ongoing evaluation of the geologic hazards associated with eight frozen debris lobes identified along a 30km stretch of the Dalton Highway (Figure 1B). These studies include the collection of multi-date differential GPS data to help understand the style and rate of frozen debris lobe movement (Daanen et al., 2012; Darrow et al., 2012), and a preliminary frozen debris lobe geologic classification scheme (Hubbard, 2013). This study evaluates the geologic and geomorphic characteristics of the frozen debris lobe catchment areas which is an important component in understanding the hazard potential of the frozen debris lobes.

The objectives of this study are to:

- 1) Map bedrock geology at a large scale to improve our understanding of the lithologic variations in the bedrock geology.
- 2) Describe and document the geomorphology and active slope processes.

3. BACKGROUND

BEDROCK

The surficial and bedrock geology of the south-central Brooks Range has been previously mapped at scales of 1:250,000 (Brosge & Reiser, 1964; Hamilton, 1978; Brown and Kreig, 1983) and 1:63,360 (Hamilton, 1979; Dillon et al., 1988; Dillon and Reifensuhl, 1995). For the purposes of this study, larger scale, higher resolution geologic mapping of the frozen debris lobe catchments was needed to identify lithologic variations within the catchments to understand how those variations affect debris contribution to the frozen debris lobes.

GEOMORPHOLOGY

Hamilton (1978) was the first to recognize and map the frozen debris lobes as active lobate mass wasting features, which he called flow slides. Other authors mapped the frozen debris lobes as mostly inactive rock glaciers (Kreig and Reger, 1982; Brown and Kreig, 1983), glacial drift and morainal deposits (Brosge & Reiser, 1964), and as undifferentiated colluvial deposits (Dillon, et al., 1988). Frozen debris lobes can be described as permafrost-regulated, actively moving, elongate, frozen mass movement features found on mountain slopes that are comprised primarily of frozen soil, rock, and debris. These features move down slope by a variety of gravity driven mechanisms, including permafrost creep, basal sliding, and active layer movement such as gelifluction and sliding of frozen slabs (Daanen et al., 2012; Darrow et al., 2012).

4. METHODS

ArcGIS was used to visualize and analyze multi-date remotely sensed imagery, including LiDAR-derived data such as DEMs, hillshades (Figure 2), slope maps, and contours; AHAP (Alaska High Altitude Photography); and satellite photography. Catchment area boundaries for each frozen debris lobe were delineated using the ArcGIS Watershed Spatial Analyst Tool and LiDAR DEMs.

Field work conducted during June and August of 2013 consisted of traversing ridges that defined catchment boundaries (Figure 3) in order to map geologic contacts and collect, describe, and identify rock samples. Catchment area geomorphology and active slope processes were visually identified during traverses and documented with GPS, photography, and videography. All collected field data (GPS points, photos, sample sites, and note locations) were managed in ArcGIS and Excel.

Catchment area geologic maps were digitized in ArcGIS. Multiple datasets were utilized in the generation of catchment area geologic maps, including existing geologic maps, field observations and rock sample identification and LiDAR-derived hillshades, contours, and slope maps. These data were used for refining placement of geologic contacts and to extrapolate contacts beyond observation points.

Figure 3. Bedrock ridge on the southern catchment boundary of FDL-11.

5.1. LiDAR IMAGERY

In 2011 DGGS acquired high resolution LiDAR data for an area of ~7,700 square kilometers along proposed natural gas pipeline routes (Hubbard et al., 2011). This LiDAR data encompasses many of the frozen debris lobe catchment areas adjacent to the Dalton Highway and provides a high resolution dataset useful for geologic mapping, especially in areas of heavy vegetation where access is difficult and aerial photography is ineffective.

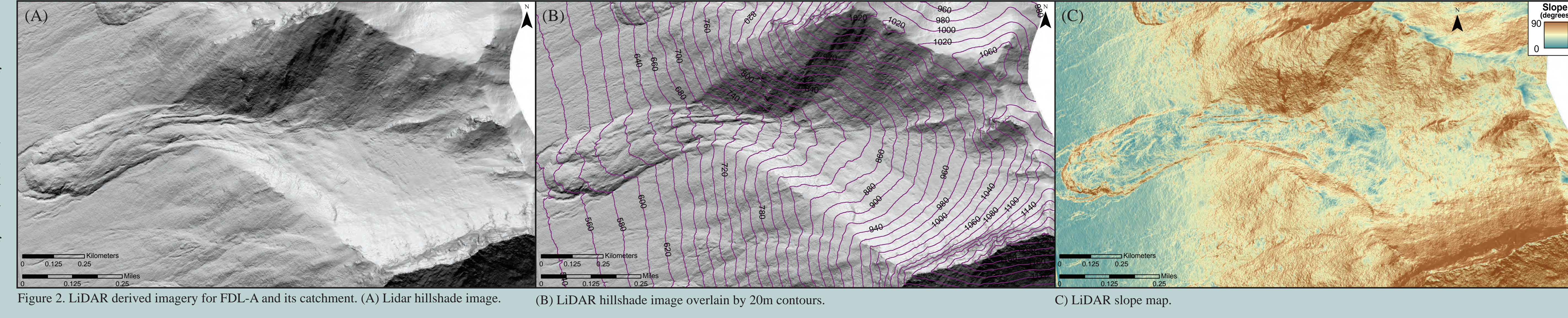


Figure 2. LiDAR derived imagery for FDL-A and its catchment. (A) Lidar hillshade image. (B) Lidar hillshade image overlain by 20m contours. (C) LiDAR slope map.

5. DATA & RESULTS

5.2. FDL- A, -B & -C

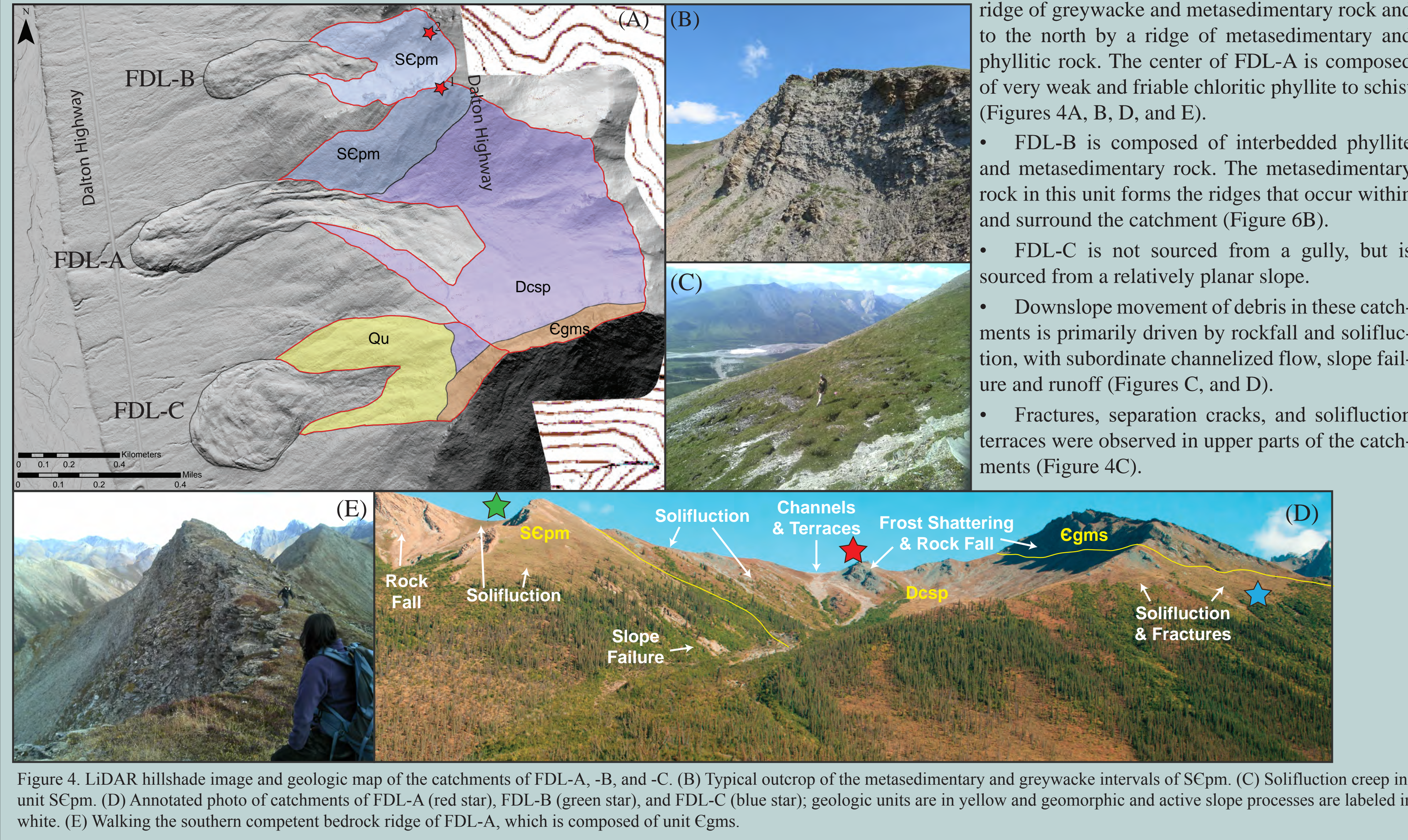


Figure 4. LiDAR hillshade image and geologic map of the catchments of FDL-A, -B, and -C. (B) Typical outcrop of the metasedimentary and greywacke intervals of SCpm. (C) Solifluction creep in unit SCpm. (D) Annotated photo of catchments of FDL-A (red star), FDL-B (green star), and FDL-C (blue star); geologic units are in yellow and geomorphic and active slope processes are labeled in white. (E) Walking the southern competent bedrock ridge of FDL-A, which is composed of unit Egms.

LEGEND

QUATERNARY DEPOSITS		LOWER PALEOZOIC METASEDIMENTARY ROCKS																																													
Qu	Undifferentiated Quaternary deposits.	Olks	Platy to massive, brown and gray limestone.																																												
DEVONIAN METASEDIMENTARY AND METAVOLCANIC ROCKS		Op	Platy, black phyllite.																																												
Dsp	Predominantly dark gray to black and brown slate and phyllite; subordinate interbedded graphitic phyllite and metasilstone to metasediment.	Egms	Interbedded platy to massive, gray-brown to green greywacke, metasediment and metasilstone.																																												
Dls	Massive, dark gray limestone interbedded with thin, platy, black phyllite.	SCpm	Predominantly interbedded platy, brown to gray-black phyllite, metasilstone, metasediment and greywacke; subordinate slate.																																												
Ds	Predominantly gray and black slate; subordinate phyllite.	Catchment area boundaries																																													
Dcsp	Predominantly interbedded platy, purple and green-blue chloritic schist and phyllite subordinate black to gray phyllite.	*Unit age designations based on previous geologic maps and reports (Brosge and Reiser, 1964; Hamilton, 1978; Dillon et al., 1988; Dillon and Reifensuhl, 1995).																																													
Dhbc	Platy to massive, black to green metasilstone to metasediment.	Point Load Index Test Results (Table 1)																																													
Dbp	Platy, brown to black phyllite; previously mapped as the Hunt Fork Shale (Hamilton, 1978; 1979; Dillon, 1988).	The point load index test was used here to determine the uniaxial compressive strength of ten collected samples (Figures 4, 5; and 6). It should be noted, however, that the point load index test is not recommended for platy or weak rocks, and that most of the collected samples fall into this category. Given this caveat, these results do illustrate that all of the tested samples are fairly weak.																																													
DEVONIAN IGNEOUS AND THERMALLY METAMORPHOSED ROCKS		<table border="1"> <thead> <tr> <th>Sample #</th> <th>σ₁ (psi)</th> <th>σ₂ (MPa)</th> <th>FDL #</th> </tr> </thead> <tbody> <tr><td>1</td><td>7308.52</td><td>50.40</td><td>FDL-A</td></tr> <tr><td>2</td><td>11210.87</td><td>77.32</td><td>FDL-B</td></tr> <tr><td>3</td><td>4977.31</td><td>34.33</td><td>FDL-D</td></tr> <tr><td>4</td><td>4762.68</td><td>32.85</td><td>FDL-D</td></tr> <tr><td>5</td><td>3731.51</td><td>25.73</td><td>FDL-D</td></tr> <tr><td>6</td><td>2207.61</td><td>15.22</td><td>FDL-D</td></tr> <tr><td>7</td><td>2987.07</td><td>20.60</td><td>FDL-D</td></tr> <tr><td>8</td><td>6637.44</td><td>45.78</td><td>FDL-D</td></tr> <tr><td>9</td><td>7648.91</td><td>52.75</td><td>FDL-11</td></tr> <tr><td>10</td><td>5844.50</td><td>40.31</td><td>FDL-11</td></tr> </tbody> </table>		Sample #	σ ₁ (psi)	σ ₂ (MPa)	FDL #	1	7308.52	50.40	FDL-A	2	11210.87	77.32	FDL-B	3	4977.31	34.33	FDL-D	4	4762.68	32.85	FDL-D	5	3731.51	25.73	FDL-D	6	2207.61	15.22	FDL-D	7	2987.07	20.60	FDL-D	8	6637.44	45.78	FDL-D	9	7648.91	52.75	FDL-11	10	5844.50	40.31	FDL-11
Sample #	σ ₁ (psi)	σ ₂ (MPa)	FDL #																																												
1	7308.52	50.40	FDL-A																																												
2	11210.87	77.32	FDL-B																																												
3	4977.31	34.33	FDL-D																																												
4	4762.68	32.85	FDL-D																																												
5	3731.51	25.73	FDL-D																																												
6	2207.61	15.22	FDL-D																																												
7	2987.07	20.60	FDL-D																																												
8	6637.44	45.78	FDL-D																																												
9	7648.91	52.75	FDL-11																																												
10	5844.50	40.31	FDL-11																																												
Dim	Platy to massive, green to dark gray and black igneous and metamorphic calcite-rich rocks; previously mapped as diabase, gabbro, and diorite sills; and tremolite skarn, calc-silicate hornfels, and siliceous hornfels (Hamilton, 1978; 1979; Dillon, 1988).	* Point load index sample location																																													

5.3. FDL-D

- The catchment of FDL-D is flanked to the south by a resistant ridge of limestone and to the north by a prominent ridge of igneous and metamorphic rocks (Figures 5A, B, and F).
- The center of the catchment consists of three different lithologic units varying from slate to phyllite to platy limestone (Figures 5A, B, D, and E).
- Geologic units within the catchment trend roughly parallel to the flow direction of FDL-D (Figure 5A).
- Downslope movement of debris is primarily driven by solifluction, and rock fall of frost shattered material (Figure 5C, D, and E).
- Slope failures are common in the lower part of the catchment area near the frozen debris lobe (Figure 5C).
- Standing water and fractures were observed in the upper parts of the catchment area within unit Dim.

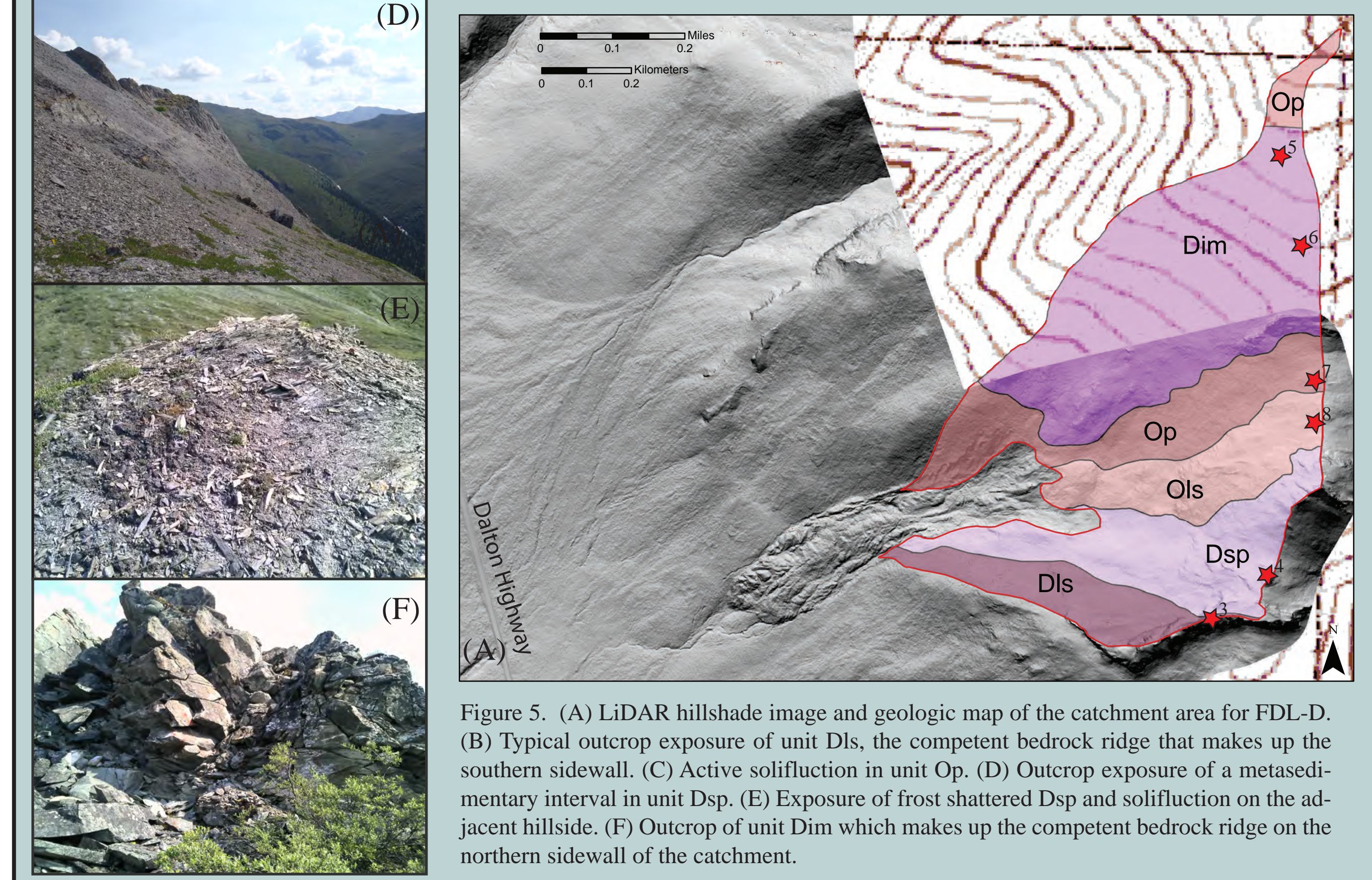


Figure 5. (A) LiDAR hillshade image and geologic map of the catchment area for FDL-D. (B) Typical outcrop exposure of unit Dis, the competent bedrock ridge that makes up the southern sidewall. (C) Active solifluction in unit Op. (D) Outcrop exposure of a metasedimentary interval in unit Dsp. (E) Exposure of frost shattered Dsp and solifluction on the adjacent hillside. (F) Outcrop of unit Dim which makes up the competent bedrock ridge on the northern sidewall of the catchment.

5.4. FDL- 11

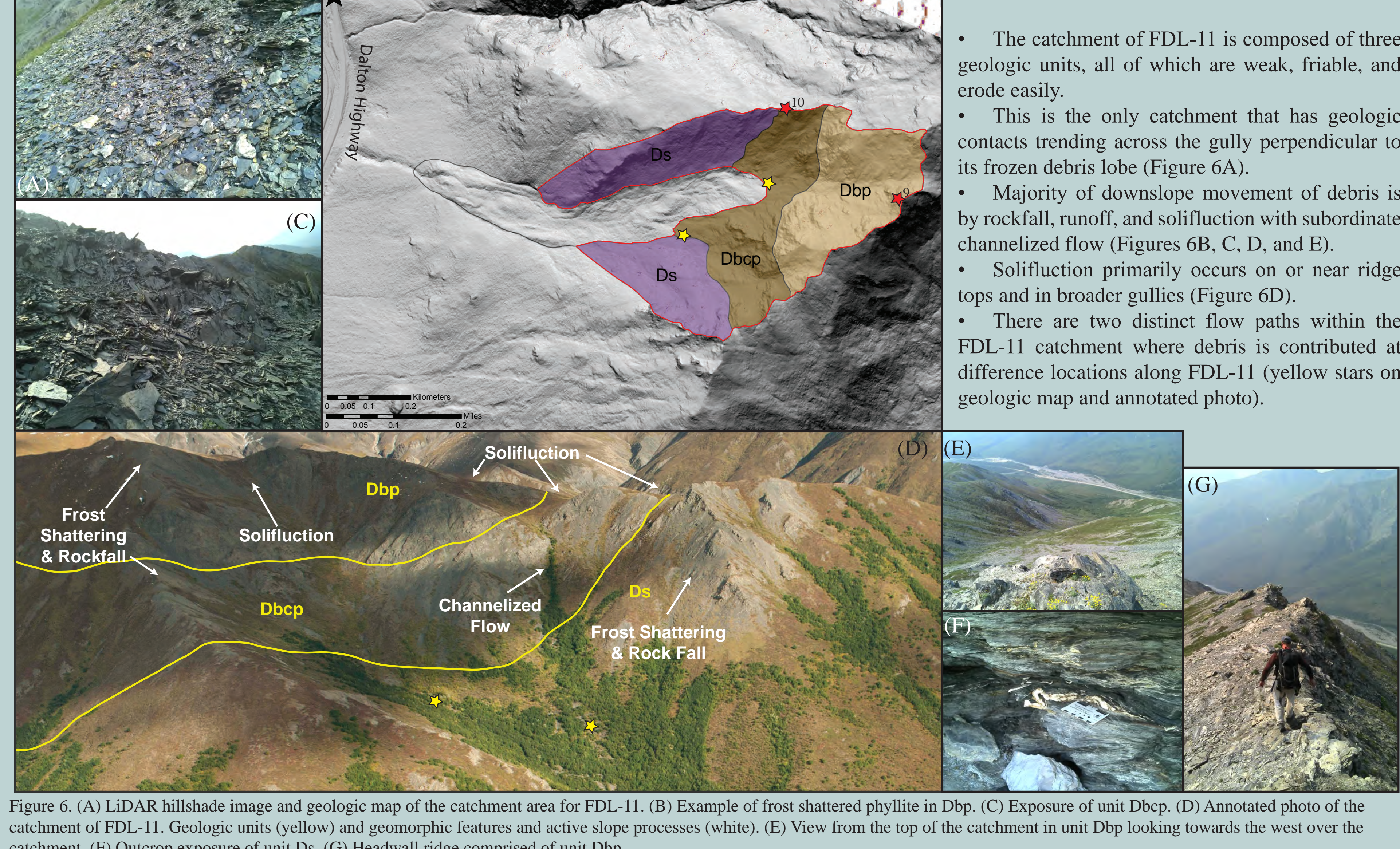


Figure 6. (A) LiDAR hillshade image and geologic map of the catchment area for FDL-11. (B) Example of frost shattered phyllite in Dbp. (C) Exposure of unit Dhbc. (D) Annotated photo of the catchment of FDL-11. Geologic units (yellow) and geomorphic features and active slope processes (white). (E) View from the top of the catchment in unit Dhbc looking towards the west over the catchment. (F) Outcrop exposure of unit Ds. (G) Headwall ridge comprised of unit Dbp.

6. DISCUSSION

Geologic mapping revealed that three of the five catchments examined (FDL-A, -B, and -D) have geologic contacts that trend parallel to the long axis of the debris lobes (roughly E-W) and coincide with the steep resistant bedrock ridges of limestone, greywacke, metasedimentary and igneous rocks that make up the sidewalls of the catchment gullies. In the central and headwall parts of these catchments, between the resistant bedrock ridges, are geologic units comprised of less resistant, platy, and friable material such as chloritic schist, phyllite, and slate. The resistant bedrock ridges that make up the sidewalls confine the weaker, platier, and more friable units. Eroded debris within the catchments is generally focused towards the of the gully and converges between the confining ridges near the top of the frozen debris lobe.

In the FDL-11 catchment, geologic contacts trend perpendicular to the long axis of the frozen debris lobe (roughly N-S across the catchment) and near the headwall of the catchment is a contact between a more competent unit of phyllite and a less competent unit of metasilstone and metasediment (Table 1). Because FDL-11 is not confined by two ridges of resistant bedrock that focus eroded debris towards a central flow path within the catchment, there are two main flow paths within the overall catchment that contribute debris at different locations along the length of FDL-11.

Despite the differences in geologic units and variations in the nature of contacts between the examined catchments, all of the frozen debris lobes and their catchments have a key similarity: they are primarily sourced from, and occur in, geologic units where material is weak, platy, and friable relative to surrounding units.

Although solifluction creep occurs on or near most ridge tops, in areas where bedrock is composed of platy and friable material solifluction appears to be the main mechanism for downslope transport of debris. This is in contrast to areas of competent bedrock where frost shattered material is primarily transported downslope by rockfall and runoff processes.

7. SUMMARY

- Geologic mapping and geomorphic characterization of frozen debris lobe catchments was conducted at five frozen debris lobes located along the Dalton Highway Corridor.
- Catchments for FDL-A, -B, and -D are flanked to the north and south by ridges of resistant bedrock and have centers consisting of less resistant, platy, and friable rocks. In contrast, the catchment for FDL-11 is not flanked by ridges of competent bedrock, but instead a geologic contact near the catchment headwall separates more competent rocks upslope from less competent rocks that make up the catchment sidewalls. FDL-C is the only frozen debris lobe that is not sourced from a gully, but is sourced from a relatively planar slope.
- All of the examined frozen debris lobes are primarily sourced from and occur in geologic units where material is weak, platy, and friable relative to surrounding geologic units.
- Principal active slope processes transporting debris downslope include solifluction, rockfall, and runoff. Subordinate slope processes include channelized flow and slope failures.
- Solifluction creep occurs on or near most ridge tops, and is the foremost mechanism for downslope transport of debris derived from platy, weak, and friable bedrock.
- Rockfall and runoff are the primary mechanisms for downslope transport of frost shattered debris derived from competent bedrock ridges.
- Separation fractures and standing water occur in the upper parts of some catchment areas.

8. REFERENCES

Brosge, W.P. and Reiser, H.N., 1964. Geologic map and section of the Chandalar Quadrangle, Alaska. U.S. Geological Survey Miscellaneous Geologic Investigations Map 775. 1 sheet, scale 1:250,000.
 Brown, J. and Kreig, R.A., 1983. Guidebook to permafrost and related features along the Elbert and Dalton Highways, Fair to Prudhoe Bay, Alaska. Alaska Division of Geological and Geophysical Survey Guidebook, 239 p.
 Daanen, R.P., Grosse, G., Darrow, M.M., Hamilton, T.D., Jones, B.M., 2012. Rapid movement of frozen debris lobes: implications for permafrost degradation and slope instability in the south-central Brooks Range, Alaska. Natural Hazards and Earth System Sciences, v. 12, pp. 1521-1537.
 Darrow, M.M., Daanen, R.P., and Simpson, J.M., 2012. Monitoring and analysis of frozen debris lobes, Fairbanks, Alaska. Department of Transportation, University Transportation Center Program, Issue Report 11-1.
 Dillon, J.T., Hanna, A.G., Darrow, J.T., Schell, D.N., Blum, J.D., Jones, D.L., and Howell, D.G., 1988. Preliminary geologic map and section of the Chandalar D-6 and parts of the Chandalar C-6 and Wascott C-1 and D-1 quadrangles, Alaska. Alaska Division of Geological & Geophysical Surveys Report of Investigation 88-5. 1 sheet, scale 1:63,360.
 Dillon, J.T. and Reifensuhl, R.B., 1995. Geologic map of the Chandalar C-6 Quadrangle, south-central Brooks Range, Alaska. Alaska Division of Geological & Geophysical Surveys Professional Paper 95-1. 1 sheet, scale 1:63,360.
 Hamilton, T.D., 1978. Surface geologic map of the Chandalar Quadrangle, Alaska. U.S. Geological Survey Miscellaneous Field Studies Map 878-A. 1 sheet, scale 1:250,000.
 Hamilton, T.D., 1979. Geologic map of Alaska, Fairbanks area, Alaska, June-August 1975. U.S. Geological Survey Open-File Report 79-27, 64 p., 4 sheets.
 Hubbard, T.D., Kretzler, R.D., and Goulet, R.A., 2011. High-resolution lidar data for Alaska: determining catchment boundaries. U.S. Geological Survey Open-File Report 2011-3, 29 p.
 Hubbard, T.D., Spangler, E., Daanen, R., Darrow, M., Simpson, J., and Southerland, L., 2013. Frozen debris lobes - characterizing a potential geologic hazard along the Dalton Highway, southern Brooks Range, Alaska. Geological Society of America Abstracts with Programs, v. 45, no. 7, p. 152.
 King, R.A. and Reiser, H.N., 1982. Aerial photo analysis and summary of landform and properties along the route of the trans-Alaska pipeline system, Alaska. Alaska Division of Geological and Geophysical Survey Report 66, 149 p.

9. THANKS...

This work was supported by a State of Alaska Capital Improvements Project with additional support from the University of Alaska Fairbanks. The permission to access areas granted by Alyeska Pipeline Service Company, and U.S. Bureau of Land management was greatly appreciated. The skilled work of our helicopter pilots helped make access to our field areas possible.